Solar Energy Materials & Solar Cells 165 (2017) 119–127

Contents lists available at ScienceDirect

Solar Energy Materials & Solar Cells

journal homepage: www.elsevier.com/locate/solmat

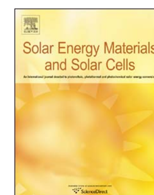

Systematic survey of suitable buffer and high resistive window layer materials in $CuIn_{1-x}Ga_xSe_2$ solar cells by numerical simulations

Andreas Bauer*, Samaneh Sharbati, Michael Powalla

Zentrum für Sonnenenergie- und Wasserstoff-Forschung Baden-Württemberg, Industriestr. 6, D-70565 Stuttgart, Germany

ARTICLE INFO

Keywords:
CIGS
Numerical simulation
Buffer layer
Window layer
Zinc magnesium oxide

ABSTRACT

This work investigates the impact of opto-electronical buffer (b) and high resistive window layer (w) properties, i.e. band gap E_g(b, w) and electron affinity χ_e(b, w), on the device performance of chalcopyrite $CuIn_{1-x}Ga_xSe_2$ (CIGS) solar cells by numerical simulations with SCAPS. We established an initial device model based on an experimental device and its *J–V*, *C–V*, and EQE data at room temperature as well as its quantified depth profile for the [Ga]/([Ga]+[In]) ratio (GGI). The device features a non-uniform CIGS doping profile as well as a strongly doped CIGS surface layer. Based on our simulations that include various buffer layer materials, we argue that the most suitable buffer *and* window layer is $Zn_{1-z}Mg_zO$. The potential gain in efficiency is up to 0.9% absolute which corresponds to a relative gain of 4.1%.

1. Introduction

Several independent research institutes, NREL, EMPA and ZSW, already achieved more than 20% power conversion efficiency with thin-film $CuIn_{1-x}Ga_xSe_2$ (CIGS) solar cells [1–3]. The former CIGS thin-film solar cell world record value of 22.3% was achieved by Solar Frontier [4] in 2015 but recently surpassed by ZSW on 0.5 cm^2 with 22.6% [3].

Alternative buffer materials for the commonly utilized CdS have been under investigation for a long time as summarized in [5–7], primarily in order to enhance photo-current generation due to their wider band gap compared to CdS. Among materials that match these criteria are $ZnO_{1-y}S_y$ (here: ZOS(y)) [8–12], ZnSe [13], $ZnIn_ySe_{\tilde{y}}$ [14], $Zn_{1-y}Mg_yO$ (here: ZMO(y)) [15,16], In_2S_3 [17], and In_2Se_3 [18]. These materials have demonstrated that results comparable to CdS can be achieved, e.g. by ZOS(y) with an efficiency of 21.0% [19]. Hultqvist et al. reported an efficiency of 18.1% for a CIGS solar cell with an atomic-layer-deposited ZMO(y) buffer layer, presently the highest value for this material combination [20]. With In_2S_3, the highest efficiency of 18.2% was achieved in 2016 [21].

Marlein et al. [22] experimentally compared CdS, In_2S_3, and ZMO(z) as buffer layer materials and used numerical simulations with SCAPS [23] to interpret the experimental results. Chelvanathan et al. [24] also restricted their buffer layer investigation to some selected materials where the focus was on buffer layer thickness and the efficiency's temperature coefficient. Recently, another theoretical study investigated favorable material parameters specifically for the combination of ZOS(y) and ZMO(z) in a buffer/window layer stack [25].

For our study by numerical simulations, we initially choose a completely material-independent approach by restricting it to two key parameters: buffer (b) and window layer (w) band gaps (E_g(b, w)) and electron affinities (χ_e(b, w)). In order to have a realistic basis for all simulations, we establish an initial device model based on its experimental data. Based on this experimental device model and its special features, i.e. non-uniform CIGS doping, strongly doped surface CIGS layer, and Ga-grading, we identify suitable semiconductor materials for buffer and window layer application that match the requirements indicated by our simulations. Since all results may depend on the CIGS layer's electron affinity, i.e. its [Ga]/([Ga]+[In]) ratio (GGI=x), especially at the CIGS/buffer layer interface, we review our results with respect to this subject.

2. Experimental

The basic experimental device and its structure are shown in Fig. 1a. The Mo layer is sputtered and the CIGS layer is co-evaporated by a static multi-stage process. CdS is deposited in a chemical bath and followed by sputtering $Zn_{0.8}Mg_{0.2}O$ (ZMO(0.2)) and subsequently ZnO:Al_2O_3 (ZAO). The device is completed by grid evaporation. For more process details refer to [3].

External quantum efficiency measurements were certified by Fraunhofer ISE. *J–V* characterization was carried out with a WACOM solar simulator (AM1.5G, AAA) and a four-point measurement setup at 298 K. *C–V* characterization was carried out with a HP4192A impedance

* Corresponding author.
E-mail addresses: andreas.bauer@zsw-bw.de (A. Bauer), samaneh.sharbati@semnan.ac.ir (S. Sharbati).

http://dx.doi.org/10.1016/j.solmat.2016.12.035
Received 18 August 2016; Received in revised form 5 December 2016; Accepted 19 December 2016
Available online 15 March 2017
0927-0248/ © 2016 Elsevier B.V. All rights reserved.

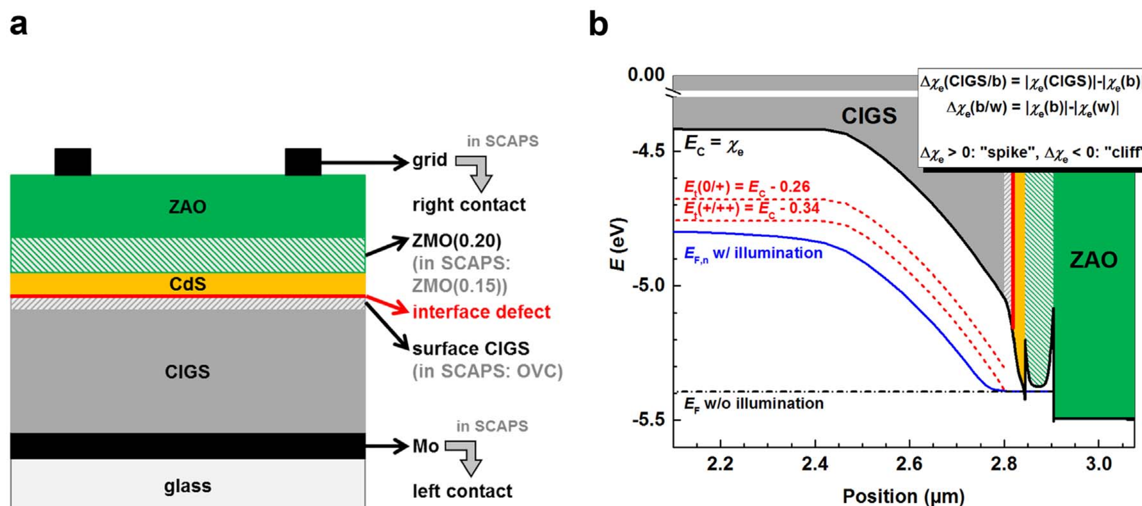

Fig. 1. Illustration of the basic experimental device: layer stack and excerpt of its band diagram as well as sign conventions for electron affinity offsets $\Delta\chi_e$. (a) Experimental and modeled basic device structure. OVC: ordered vacancy compound. (b) Excerpt of the band diagram under short circuit condition correspondent to (a) as well as the sign convention for electron affinity offset types $\Delta\chi_e$ (spike, cliff) as inset. Both $\Delta\chi_e$(CIGS/b) > 0 and $\Delta\chi_e$(b/w) > 0 indicate a spike at each buffer layer interface. Note: SCAPS uses as input absolute values.

analyzer at 298 K. Compositional CIGS depth profiles were recorded with a GDOES profiler (glow discharge optical emission spectroscopy, Horiba, Yvon), quantified by XRF measurements (EDAX EAGLE XXL).

3. Numerical modeling

A model of the experimental device described above was created with the device simulation program SCAPS[1] [23]. The structure of the modeled experimental device in SCAPS is shown in Fig. 1a. However, a lower Mg content (z=0.15) is chosen for the modeled device for consistency reasons.[2] Table 1 summarizes all model parameters used in this work. Fig. 1b shows the corresponding band diagram (excerpt) and sign conventions for electron affinity offsets $\Delta\chi_e$ (positive: spike, negative: cliff). Most of the parameters are taken from the literature except for parameters highlighted in bold font which were determined either by fitting the simulation to measurement data or directly from measurement data. Figs. 2 show the device's GGI profile and compare measurement data to simulated J–V (w/o, w/ illumination), EQE, and Mott–Schottky curves. The real device comprises a graded CIGS layer so that E_g and χ_e vary with the position-dependent [Ga]/([Ga]+[In]) ratio (GGI=x) in the device (Fig. 2a). From EQE data (Fig. 2b), we deduce the minimum optical band gap (E_g) of the CIGS layer and use it to remove any potential (usually minor) GGI profile offset. This procedure ensures the correct band gap and electron affinity interpolation by SCAPS. We also use it to estimate the reflection losses at the right (front) contact and deduce the band gaps of buffer and window layers from the UV part, when possible. Mott–Schottky analysis applies to capacitance versus voltage measurements (C–V) and is a suitable method to determine doping profiles from slopes and the devices's built-in voltage from the intersection with the voltage axis (Fig. 2c). The latter is modeled by adjusting the doping concentration of the CIGS surface layer (often referred to as OVC layer (ordered vacancy compound)). Our device model features a non-uniform CIGS doping profile[3] that can be best approximated by a beta function where the surface near part of the CIGS layer is effectively weaker doped than the bulk (inset Fig. 2c). As a last step, we use the J–V data (Fig. 2d) to model additional series and shunt resistances as well as to model open-circuit voltage losses by adjusting the trap density. Igalson and Urbaniak [29] discussed that the most prominent defects under Cu-poor conditions are Cu vacancies responsible for p-type doping and In atoms on Cu sites which form compensating donor-type defects. The ratio between doping concentration in the CIGS layer and the donor defect density can be estimated to be about 100:1 [29,30], as it is also the case in our model. The resulting elementary device parameters, open-circuit voltage (V_{OC}), short-circuit current density (J_{SC}), fill factor (FF), and power conversion efficiency (η), are summarized in the inset of Fig. 2d.

Simulation and experimental data match and ensure a realistic basis for our study which validates our set of model parameters.

4. Results and discussion

Based on the model described in Section 3, we study the impact of buffer layer band gaps E_g(b) and electron affinities χ_e(b) on the device performance. Device characterization was carried out at 298 K and every simulation is done at this temperature.

The systematic window layer study focusses on a ZnO-based material, i.e. $Zn_{1-z}Mg_zO$ (ZMO(z)). ZMO(z) is used because of its wide gap that minimizes parasitic absorption, its tunable electron affinity by z and because most CIGS devices utilize it. Table 2 summarizes the range of investigated parameters.

4.1. Preliminary investigation: E_g(b), χ_e(b), and ZMO(z)

This subsection addresses the impact of buffer layer band gaps E_g(b) and electron affinities χ_e(b) with respect to window layer composition z with focus on its electron affinity χ_e(w).

Fig. 3a shows the result for a E_g(b) and χ_e(b) variation as described in Table 2 for a ZMO(0.15) window layer. For $\Delta\chi_e$(CIGS/b) in the range of ± 0.15 eV, the shape is almost symmetric and the highest efficiencies are achieved when $\Delta\chi_e$(CIGS/b) ≈ 0 eV. This result/shape is governed by the FF. The right axis also shows the corresponding χ_e(b) and the electron affinity offset $\Delta\chi_e$(b/w) between buffer and window layer (in brackets). The latter values show that the highest efficiencies can be achieved even for higher $\Delta\chi_e$(b/w) ≈ 0.2–0.4 eV.

For $\Delta\chi_e$(CIGS/b) > 0.15 eV a plateau in η appears. This plateau is a consequence of our chosen trap model in the CIGS layer. The trap states lay 0.26 eV and 0.34 eV below the conduction band and comprise a high hole capture cross section (i.e. low hole life time, cf. Fig. 1b). As

[1] Version 3.201, August 2012.

[2] This value is lower than the actual sputter target composition given in the experimental section and is due to the electronical properties (E_g(w), χ_e(w)) used in the simulation which actually correspond to 15mol% MgO.

[3] It is not clear, whether only acceptors shape the doping profile or if the acceptor concentration is constant and the shaping is due to compensating donors, e.g. by diffused Zn atoms. Therefore, the doping profile should be considered as an effective doping profile and as a mathematical but correct description.

Download English Version:

https://daneshyari.com/en/article/6457149

Download Persian Version:

https://daneshyari.com/article/6457149

Daneshyari.com